UPDATED TIDAL ENERGY FEASIBILITY RESOURCE ASSESSMENT FOR THE UNITED STATES

Alexandra Muscalus[1] and Kevin Haas
Georgia Institute of Technology
Civil and Environmental Engineering
Atlanta, GA USA

Levi Kilcher and Heidi Tinnesand
National Renewable Energy Laboratory
Golden, CO, USA

[1]Corresponding author: amuscalus@gatech.edu

INTRODUCTION

In order to evaluate the potential of any new source of energy, resource assessments are required to determine its total potential and the feasibility of energy extraction. Therefore, resource assessments are a vital part of determining the feasibility of hydrokinetic tidal energy extraction for a particular region, designing the project layout, and ultimately providing the projected annual energy production (AEP). The particular method and tools required for such resource assessments depend on the scope (feasibility or design) as well as the scale of the project.

To help clarify the types of resource assessments, the International Electrotechnical Commission (IEC) has defined a conceptual framework for assessing marine hydrokinetic resources [1] which the United States Department of Energy has adopted [2]. The overall assessment process considers resources in three stages: theoretical, technical and practical. The theoretical resource consists of the hydrokinetic energy available for conversion without consideration of any turbine properties. In essence, this is the power within the undisturbed flow field. The technical resource is the amount of power that can be generated considering the particular technology to be utilized. Specifically, technical resource assessment incorporates turbine efficiencies and interactions with the flow field to produce resource estimates that are a fraction of the theoretical resource. Finally, the practical resource takes into consideration additional restrictions of turbine operation, such as regulatory, environmental, economic, and life cycle constraints.

Feasibility studies tend to fall in the category of theoretical resource assessments as they are used to determine the upper bound of the available energy for particular regions. This paper presents a review of the methodology for feasibility studies and describes the sensitivity of results to calculation methods and location selection.

CONCEPTS OF FEASIBILITY RESOURCE ASSESSMENTS

The first step in developing any tidal energy project is to identify potential project site locations - in other words, performing regional feasibility studies to find areas with strong tidal currents. Regional feasibility studies generally use numerical simulations for determining the tidal flow conditions within particular bays or estuaries. The IEC technical specification for tidal energy resource assessments [3] provides guidance suggesting that feasibility studies may be computed using depth averaged 2D (or full 3D) models with computational grid point spacing no greater than 500 m. However, the specification does not provide guidance as to how to interpret the model data for the analysis of project feasibility.

In general, the tidal current model data from these feasibility studies may be used generically to identify geographic regions with sufficiently large currents to be of interest for tidal energy projects. The predicted current velocities from these studies may be used to estimate the AEP following the guidance in the IEC technical specification [3], although with a high level of uncertainty. Furthermore, this type of assessment is insufficient to estimate power potential for projects that have large turbine arrays relative to the cross-sectional area of the flow field, commonly a channel. Vennell

et al. [4] suggests that any array with total swept area larger than 2-5% of the cross-sectional area may be defined as large. For these large projects, the energy dissipation of the turbines and the back effect must be considered.

An illustration of the energy dissipation effect is shown in Figure 1, which demonstrates that adding more turbines will decrease the residual available kinetic power density, resulting in less overall power produced by each individual turbine. Also, there will be some threshold where adding more turbines will decrease the total power output from the full array, thereby leading to a maximum possible power that may be extracted.

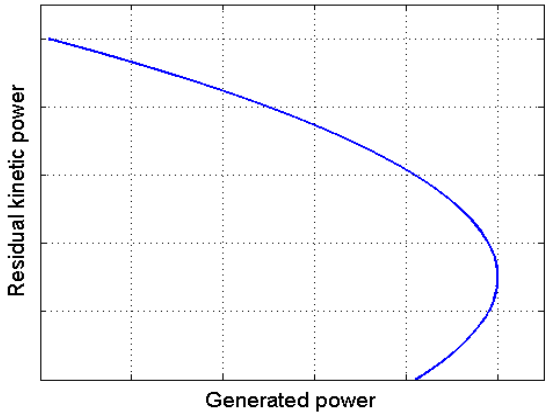

FIGURE 1: ILLUSTRATION OF THE EFFECT OF DIMINISHING RETURNS FROM ADDING ADDITIONAL TURBINES TO A CHANNEL. STARTING FROM THE TOP LEFT, AS MORE TURBINES ARE ADDED, THE RESIDUAL KINETIC POWER DECREASES AND THE GENERATED POWER INCREASES. THERE IS AN OPTIMAL POINT WHERE GENERATED POWER IS MAXIMIZED, BEYOND WHICH THE GENERATED POWER IS DECREASED AS MORE TURBINES ARE ADDED

Therefore, feasibility studies frequently use the data from tidal models in conjunction with theoretical analysis of the maximum extractable power to produce the AEP estimate. While these theoretical analyses account for the various effects that the turbines have on the flow field, they require simplifying assumptions. Still, they do produce a more reasonable estimate of the upper bound of the energy potential than analyses of the undisturbed velocities alone.

Garrett and Cummins [5], hereafter referred to as G&C, identified the significance of the back effect, a pressure induced head differential created by the obstructions in the channel. This effect increases the pressure differential driving the flow and enhances the current velocity. G&C investigated the idealized case of a tidal fence consisting of turbines across the entire cross-section of a constricted channel connecting two large bodies of water in which the tides at both ends are assumed to be unaffected by the currents through the channel. For this situation, a general formula gives the maximum average power to be between 20% and 24% of the peak tidal pressure head times the peak of the undisturbed mass flux through the channel, independent of the location of the turbine fences along the channel. The maximum average tidal stream power, P_{max}, for a single sinusoidal constituent is given as

$$P_{max} = \gamma \cdot \rho \cdot g \cdot a \cdot Q_{max} \qquad (1)$$

where γ is a parameter representing the 20 to 24% of the peak tidal pressure head, ρ is the density of seawater, g is acceleration of gravity, a is the amplitude of the tidal water level constituent, and Q_{max} is the maximum corresponding flow rate.

For a background, or natural, friction dominated, nonsinusoidal (i.e. considering more than one tidal constituent) case, if data for the head and flux in the natural state are available, the maximum average power may be estimated within an error of 10% using $\gamma = 0.22$ without any need to understand the basic dynamical balance [5]. For the general case with multiple tidal constituents, a multiplying factor for equation (1) is used to account for the additional constituents $(a_1, a_2, \dots)$ given as

$$1 + \left(\frac{9}{16}\right)(r_1^2 + r_2^2 + \cdots) \qquad (2)$$

where $r_1 = \frac{a_1}{a}, r_2 = \frac{a_2}{a} \dots$, a is the amplitude of the dominant tidal constituent, and a_n is the amplitudes of the additional constituents. This upper bound on the available power ignores losses associated with turbine operation and assumes that the turbines are deployed in uniform fences with all the water at each fence passing through the turbine. In this case, Q_{max} is associated with the velocity of the dominant tidal constituent. For the cases discussed here, the dominant tidal constituent is M2.

SENSITIVITY OF FEASIBILITY RESOURCE ASSESSMENTS

The United States national tidal energy reconnaissance resource assessment [6,7] utilized numerical simulations of the tidal flows along the coast. The geographic distribution of the kinetic power density was computed and analyzed for locations of energy hot spots. However, that analysis did not provide estimates of the theoretical bounds for the power that could be extracted. Therefore, estimates of the theoretical upper bound on the total power were determined using the method by G&C, which considers both the kinetic and potential power with the exclusion of any technology specific assumptions. This method analyzes undisturbed flow field data from the model with simple methods that account for the

cumulative effect of dissipating energy to provide information on the scale of estuaries and bays.

The general analysis method and results are documented in Haas et al. [6], although the detailed methodology required for calculating the variables used in the computation based on the tidal database constituents has not been thoroughly documented. A sensitivity analysis of the computation methods for the key parameter Q_{max} used to determine P_{max}, is presented herein.

To find Q_{max}, the volume flux is computed at discrete points across a channel transect. Three different methods for computing this discrete volume flux are utilized here incorporating to different extents the inclination angle and phase of the dominant tidal constituent.

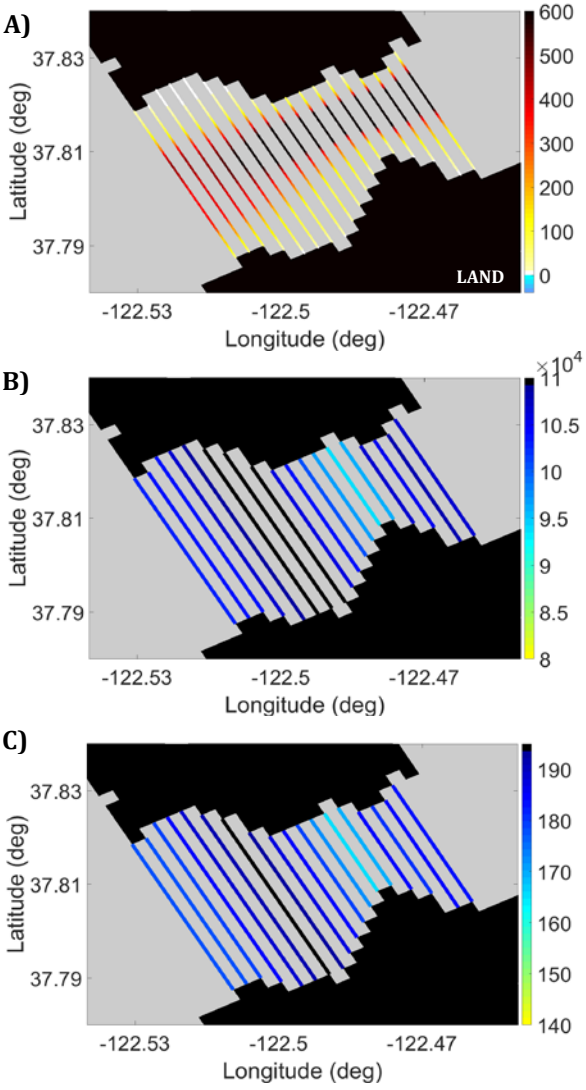

FIGURE 2: RESULTING A) DISCRETE $Q_i^{(1)}$ (m³/s), B) TOTAL Q_{MAX} (m³/s), AND C) P_{MAX} (MW) IN SAN FRANCISCO BAY FROM VELOCITY CALCULATION METHOD 1, WHICH DOES NOT INCOPORATE CONSTITUENT INCLINATION ANGLE NOR PHASE

The first method computes $Q_i^{(1)}$ for each i location using

$$Q_i^{(1)} = v_i^{ma} \cdot h_i \cdot w_i \quad (3)$$

where v_i^{ma} is the velocity amplitude of the major axis, h_i is the depth at that point, and w_i is the width along the transect of that point. Finally, Q_{max} is found as the sum of $Q_i^{(1)}$ along the transect.

Figure 2 demonstrates the results of method 1, for the Golden Gate in San Francisco Bay, CA, USA applied to 18 transects. The variation of Q_i^1 calculated at the discrete points (here, each with a w_i of ten meters) across each transect is shown in Figure 2a. The volume flux is largest in the middle where the channel is deepest and is weakest along the banks. Figure 2b shows Q_{max} and Figure 2c

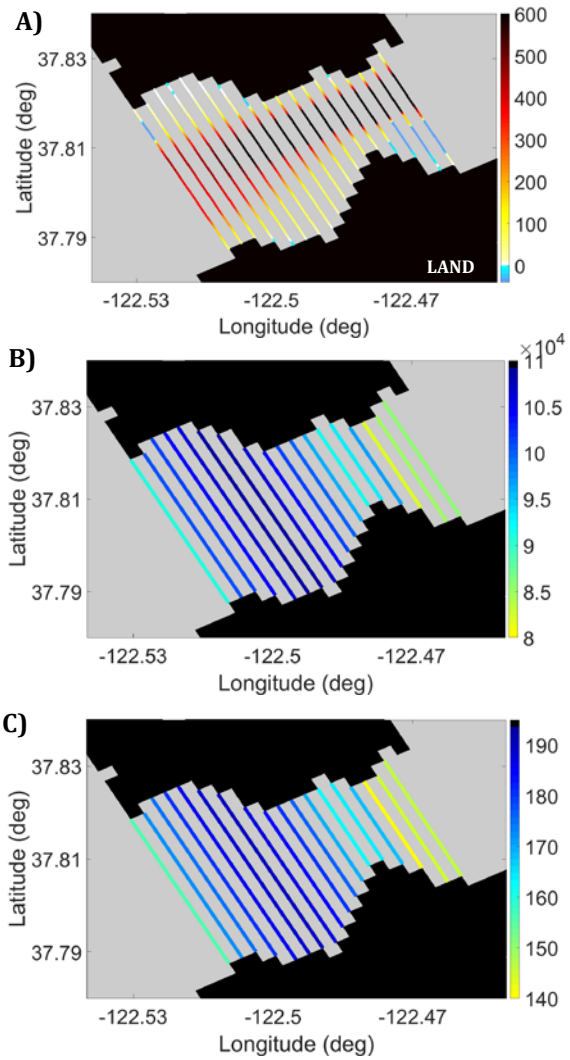

FIGURE 3: RESULTING A) DISCRETE $Q_i^{(2)}$(m³/s), B) TOTAL Q_{MAX} (m³/s), AND C) P_{MAX} (MW) IN SAN FRANCISCO BAY FROM VELOCITY CALCULATION METHOD 2, WHICH INCOPORATES CONSTITUENT INCLINATION ANGLE BUT DOES NOT ACCOUNT FOR CONSTITUENT PHASE

provides the resulting P_{max} of each transect. It is seen that the spatial variation (~10%) of P_{max} in the channel reflects that of Q_{max}.

The second method uses the approach from [6] which computes $Q_i^{(2)}$ by incorporating the inclination angle of the major axis relative to the perpendicular angle of the transect α_i using

$$Q_i^{(2)} = v_i^{ma} \cdot h_i \cdot w_i \cos(\alpha_i). \quad (4)$$

The spatial varying volume fluxes from method 2 are shown in Figure 3a. While the volume flux is obviously decreased, there are several regions with flow that opposes the primary flow direction, such as may be introduced by recirculation; points with opposing flow are shown in blue in Figure 3a. This results in several negative values, of $Q_i^{(2)}$ at discrete points that then serve to decrease the values of Q_{max} and P_{max} along transects that contain regions with opposing flow. These effects are shown in Figures 3b and 3c, which contain several transects with Q_{max} and P_{max} values that are less than those of the same transects in Figures 2b and 2c.

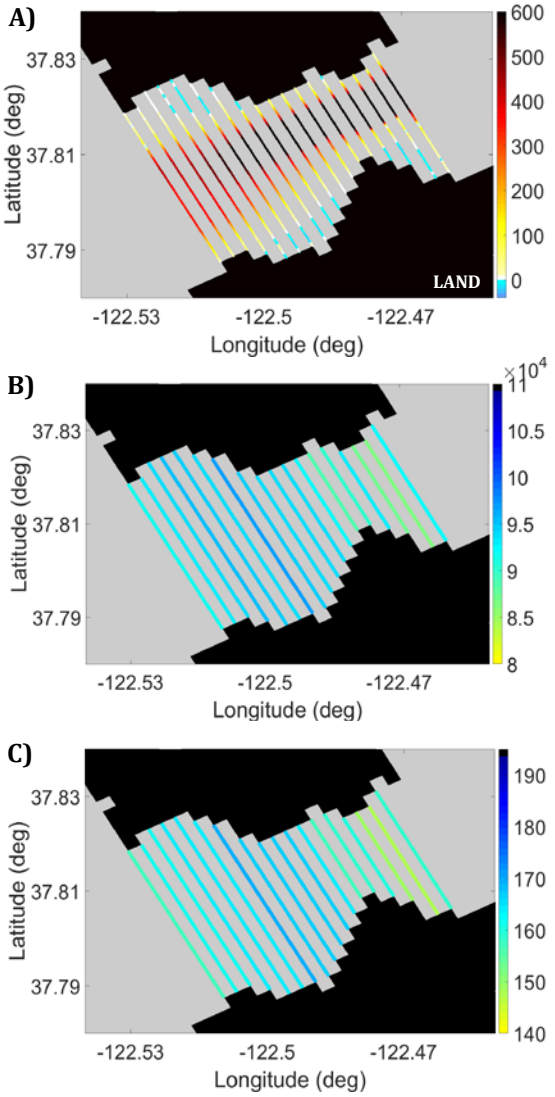

FIGURE 4: RESULTING A) DISCRETE $Q_{i,t_{max}}^{(3)}$ (m^3/s), B) TOTAL Q_{MAX} (m^3/s), AND C) P_{MAX} (MW) IN SAN FRANCISCO BAY FROM VELOCITY CALCULATION METHOD 3, WHICH INCOPORATES BOTH CONSTITUENT INCLINATION ANGLE AND PHASE

Because the flow is non-uniform across the transect, the third method incorporates the phase associated with the velocity constituent. A one month time series of the volume flux, $Q_{i,t}$, for each location is computed by using harmonic reconstruction [8] with $Q_i^{(2)}$ as the amplitude and the phases from v_i^{ma}. Next Q_{max} is found as

$$Q_{max} = MAX(\sum_{i=1}^{N} Q_{i,t}) \quad (5)$$

where N is the number of discrete locations in the transect. Finally, the spatially varying maximum volume flux, $Q_{i,t_{max}}^{(3)}$, for a transect is found by identifying the time t_{max} at which Q_{max} occurs in the time series and taking $Q_{i,t}$ at that time.

The relative phase along a transect is such that there are regions where the flow is in the opposing direction. Figure 4a highlights the increase in regions with opposing flow; as in Figure 3a, negative flow values are shown in blue. However, some of the regions shown in Figure 3a, in which the flow is reversed due to the variations in inclinations, are flipped back in Figure 4a, indicating the flow is actually in phase with the main channel. Therefore, Q_{max} is actually decreased and increased for different transects which in turn decreases or increases P_{max}.

Comparing the results of the three methods, it is observed that accounting for inclination angle and phasing produces significant effects on the resulting P_{max} values. The inclination decreases the magnitude of P_{max} between 5 and 22%, leading to a much stronger dependence on the location of the transect. However, the phase either decreases or increases the power by up to 10%, reducing the dependence of the power on transect location. Method 3 could be considered the most accurate of the methods because it accounts for both inclination angle and phasing of the tidal constituents. However, it should be noted that the across-channel variability does violate part of the assumptions in the derivation of equation (1).

SPATIAL VARIABILITY OF PMAX IN COOK INLET

The variation of P_{max} with respect to location within an inlet is examined in Cook Inlet, AK, USA. As seen in Figure 5c, P_{max} decreases from 15,000 MW at the entrance to 4,000 MW closer to end of the estuary. This illuminates what could be considered an estimate towards the technical resource assessment as energy extraction would generally not take place at the entrance but further up the estuary. Figure 5a demonstrates that the

dominant tidal amplitude increases from 1.7 meters to 2.7 meters moving inward. However, the decrease in flow rate inward, shown in Figure 5b, has a more prominent effect on P_{max}, which is presented in Figure 5c. It is clear that P_{max} is highly dependent upon Q_{max}.

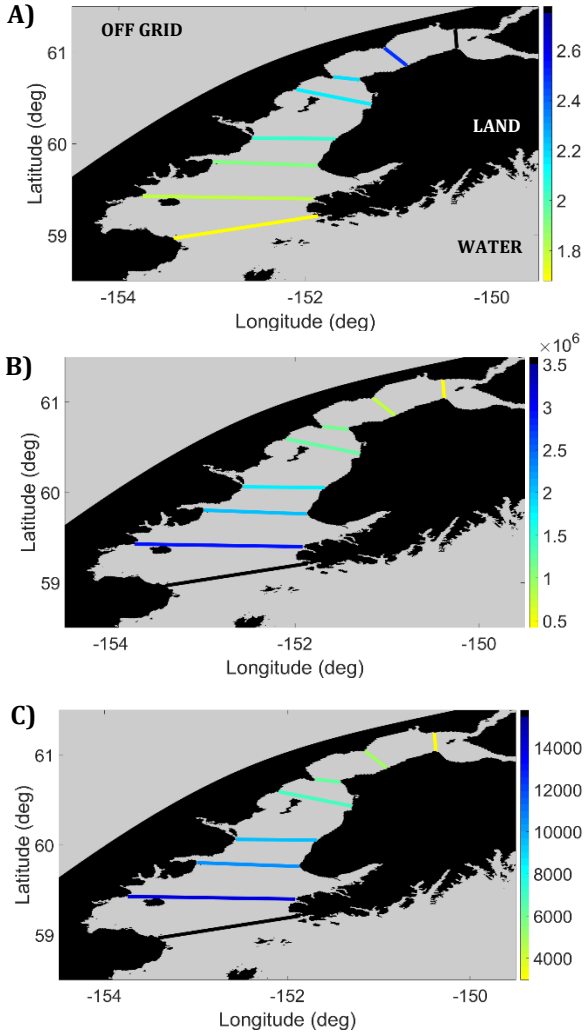

FIGURE 5: SPATIAL VARIATION OF A) M2 AMPLITUDE, B) Q_{MAX}, AND C) P_{MAX} IN COOK INLET, AK, USA

CONCLUSIONS

For realistic estuaries with complex bathymetry, when applying the G&C formulation for computing the maximum power potential, the results are sensitive to the location of the transect and the precise method for computing the parameters from the tidal water level and velocity constituents. In particular, the inclination, which generally is used when computing the volume flux in the channel, reduces the total power. However, including the relative phase of the flow across the transect can increase or decrease the total power. For the example illustrated here, the variability of the feasibility resource assessment was on the order of 10-15%. For design level tidal energy resource assessments using the IEC guidelines [3], the G&C type power estimates are used as a threshold limit for determining the required methodology. For example, one of the thresholds is when the expected energy extraction for the design is expected to exceed 2% of the theoretical limit based on G&C; therefore, the variability shown here could directly affect the design level resource assessment requirements.

ACKNOWLEDGEMENTS

Thanks to the Marine Energy Council for their guidance, support and feedback on this work. Thanks to the U.S. Department of Energy for funding this work under contract number DE-AC36-08GO28308. Georgia Tech was funded by the Alliance for Sustainable Energy, LLC, Managing and Operating Contractor for the National Renewable Energy Laboratory for the U.S. Department of Energy under subcontract number XHQ-7-70094-01.

REFERENCES

[1] International Electrotechnical Commission (IEC), 2011, "Marine energy - Wave, tidal and other water current converters - Part 1: Terminology," Technical Specification No. 62600-1:2011, IEC, Geneva, Switzerland.

[2] National Research Council (NRC), 2013, "An Evaluation of the U.S. Department of Energy's Marine and Hydrokinetic Resource Assessments," The National Academies Press, DOI 10.17226/18278, Washington, D.C.

[3] International Electrotechnical Commission (IEC), 2015, "Marine energy - Wave, tidal and other water current converters - Part 201: Tidal energy resource assessment and characterization," Technical Specification No. 62600-201:2015, IEC, Geneva, Switzerland.

[4] Vennell, R., Funke, S. W., Draper, S., Stevens, C., and Divett, T., 2015, "Designing large arrays of tidal turbines: A synthesis and review," Renewable and Sustainable Energy Reviews, Vol. 41, pp. 454-472.

[5] Garrett, C., and Cummins, P., 2005, "The power potential of tidal currents in channels," Proceedings of the Royal Society of London A: Mathematical, Physical and Engineering Sciences, Vol. 461, No. 2060, pp. 2563-2572.

[6] Haas, K. A., Fritz, H. M., French, S. P., Smith, B. T., and Neary, V., 2011, "Assessment of energy production potential from tidal streams in the United States," Final Project Report No. DE-FG36-08GO18174, Georgia Tech Research Corporation, Atlanta, GA.

[7] Defne, Z., Haas, K. A., Fritz, H. M., Jiang, L., French, S. P., Shi, X, Smith, B., Neary, V. and Stewart, K. M., 2012, "National geodatabase of tidal stream power resource in USA," Renewable and Sustainable Energy Reviews, Vol. 16, Issue 5, pp. 3326-3338.

[8] R. Pawlowicz, B. Beardsley, and S. Lentz, 2002, "Classical tidal harmonic analysis including error estimates in MATLAB using T_TIDE", Computers and Geosciences, Vol. 28, pp. 929-937.